Human hippocampal theta power indicates movement onset and distance travelled

Daniel Bush[a,b,1,2], James A. Bisby[a,b,1], Chris M. Bird[c,1], Stephanie Gollwitzer[b,d], Roman Rodionov[b], Beate Diehl[b,e], Andrew W. McEvoy[b], Matthew C. Walker[b], and Neil Burgess[a,b,2]

[a]Institute of Cognitive Neuroscience, University College London, London WC1N 3AZ, United Kingdom; [b]Institute of Neurology, University College London, London WC1N 3BG, United Kingdom; [c]School of Psychology, University of Sussex, Brighton BN1 9QH, United Kingdom; [d]Department of Neurology, University Hospital Erlangen, D-91054 Erlangen, Germany; and [e]Department of Clinical Neurophysiology, National Hospital for Neurology and Neurosurgery, London WC1N 3BG, United Kingdom

Edited by Gyorgy Buzsáki, New York University Neuroscience Institute, New York, NY, and approved October 6, 2017 (received for review June 6, 2017)

Theta frequency oscillations in the 6- to 10-Hz range dominate the rodent hippocampal local field potential during translational movement, suggesting that theta encodes self-motion. Increases in theta power have also been identified in the human hippocampus during both real and virtual movement but appear as transient bursts in distinct high- and low-frequency bands, and it is not yet clear how these bursts relate to the sustained oscillation observed in rodents. Here, we examine depth electrode recordings from the temporal lobe of 13 presurgical epilepsy patients performing a self-paced spatial memory task in a virtual environment. In contrast to previous studies, we focus on movement-onset periods that incorporate both initial acceleration and an immediately preceding stationary interval associated with prominent theta oscillations in the rodent hippocampal formation. We demonstrate that movement-onset periods are associated with a significant increase in both low (2–5 Hz)- and high (6–9 Hz)-frequency theta power in the human hippocampus. Similar increases in low- and high-frequency theta power are seen across lateral temporal lobe recording sites and persist throughout the remainder of movement in both regions. In addition, we show that movement-related theta power is greater both before and during longer paths, directly implicating human hippocampal theta in the encoding of translational movement. These findings strengthen the connection between studies of theta-band activity in rodents and humans and offer additional insight into the neural mechanisms of spatial navigation.

theta | hippocampus | navigation | spatial memory | intracranial EEG

The rodent hippocampal local field potential (LFP) is dominated by 6- to 10-Hz theta oscillations during translational movement (1, 2). Both the power (1, 3) and frequency (3–6) of theta are positively correlated with running speed. Theta oscillations might therefore encode self-motion information and contribute to the generation of spatially modulated firing patterns (7–9). A critical concern for contemporary neuroscience is to establish whether this hypothesis can be translated across species. During navigation, intracranial recordings from depth electrodes in the human hippocampus have shown that theta is more prevalent during movement than during stationary periods (10–12) and that theta power increases with movement speed (13). In addition, increases in movement-related theta power are seen across the neocortex (10, 11, 14). These findings support the hypothesis that human theta oscillations might encode self-motion information. However, it has also been demonstrated that human theta-band activity typically occurs in transient bursts distributed throughout movement, in contrast to the continuous high-amplitude oscillation observed in the rodent (15, 16). Moreover, these studies identified movement-related oscillations within both higher and lower frequency theta bands (17–20). Hence, it is not yet clear how theta oscillations in the human hippocampus relate to those observed in the rodent.

To address this question, we examine intracranial recordings from the temporal lobe of presurgical epilepsy patients performing a self-paced spatial memory task (21). In contrast to previous studies, we focus on analyzing changes in oscillatory power around movement onset in the virtual environment. In the rodent hippocampal formation, theta power increases are observed during the stationary period immediately before movement initiation in both the membrane potential oscillations of single neurons (22) and in the LFP (1, 2, 23–26). In addition, magnetoencephalographic (MEG) recordings in healthy human participants have identified a transient increase in theta power around virtual movement onset that is correlated with subsequent spatial memory performance, although the source of this oscillation could not be localized (27). Here, we demonstrate that movement onset is associated with a significant increase in both low and high theta power across the human hippocampus and lateral temporal lobe that persists throughout the remainder of movement. Moreover, we find that increases in movement-related theta power are greater for longer paths, directly implicating human hippocampal theta in the encoding of translational movement. These findings support the translation of hypotheses regarding movement-related theta from rodent models and provide additional insight into the mechanisms of human spatial navigation.

Significance

Rodent hippocampal theta-band oscillations are observed throughout translational movement, implicating theta in the encoding of self-motion. Interestingly, increases in theta power are particularly prominent around movement onset. Here, we use intracranial recordings from epilepsy patients navigating in a desktop virtual reality environment to demonstrate that theta power is also increased in the human hippocampus around movement onset and throughout the remainder of movement. Importantly, these increases in theta power are greater both before and during longer paths, directly implicating human hippocampal theta in the encoding of translational movement. These findings help to reconcile previous studies of rodent and human hippocampal theta oscillations and provide additional insight into the mechanisms of spatial navigation in the human brain.

Author contributions: C.M.B. and N.B. designed research; D.B., J.A.B., C.M.B., S.G., R.R., B.D., A.W.M., M.C.W., and N.B. performed research; D.B., J.A.B., S.G., and R.R. analyzed data; D.B., J.A.B., C.M.B., S.G., R.R., B.D., A.W.M., M.C.W., and N.B. wrote the paper; B.D. supervised patients; and A.W.M. performed surgeries.

The authors declare no conflict of interest.

This article is a PNAS Direct Submission.

[1]D.B., J.A.B., and C.M.B. contributed equally to this work.

[2]To whom correspondence may be addressed. Email: drdanielbush@gmail.com or n.burgess@ucl.ac.uk.

This article contains supporting information online at www.pnas.org/lookup/suppl/doi:10.1073/pnas.1708716114/-/DCSupplemental.

Results

Behavioral Data. Nineteen presurgical epilepsy patients with depth electrodes implanted in the temporal lobe performed a spatial memory task in a virtual reality (VR) environment (Fig. 1*A*) (21, 27, 28). Temporal lobectomy patients have been shown to be impaired on a similar task (29), and performance of this task has been related to increases in hippocampal activity in previous fMRI studies (21, 27). Briefly, during encoding, patients were asked to navigate toward and memorize the location of four visible objects. During retrieval, patients were cued with an image of one object and then placed back in the environment and asked to navigate toward the remembered location of that (now invisible) object and make a response. This provides a continuous measurement of distance error, Δd, between the location at which the patient made a response and the true location of the object in each retrieval trial. The object then appeared in its correct location to provide patients with feedback on their performance and allow further learning. The feedback period ended when patients navigated to the location of the now-visible object.

Three patients did not complete the task due to technical difficulties, one patient could not perform the task, and two patients failed to produce sufficient stationary periods due to continuous movement. For the remaining 13 patients (see Tables S1 and S2 for details), mean $\Delta d = 28.7 \pm 14.4$ virtual meters (vm) (range, 10.5–49.6 vm), which is smaller than chance performance [~49.4 vm, $t(12) = -5.19$, $P < 0.001$, Cohen's $d = 1.44$] (Fig. 1 *B* and *C*). In addition, there was a significant reduction in Δd for each object across retrieval trials [$t(12) = -2.25$, $P < 0.05$, $d = 0.62$] (Fig. 1*D*), suggesting that the feedback provided at the end of each trial led to an improvement in patient's performance. These results indicate that patients could successfully perform the task.

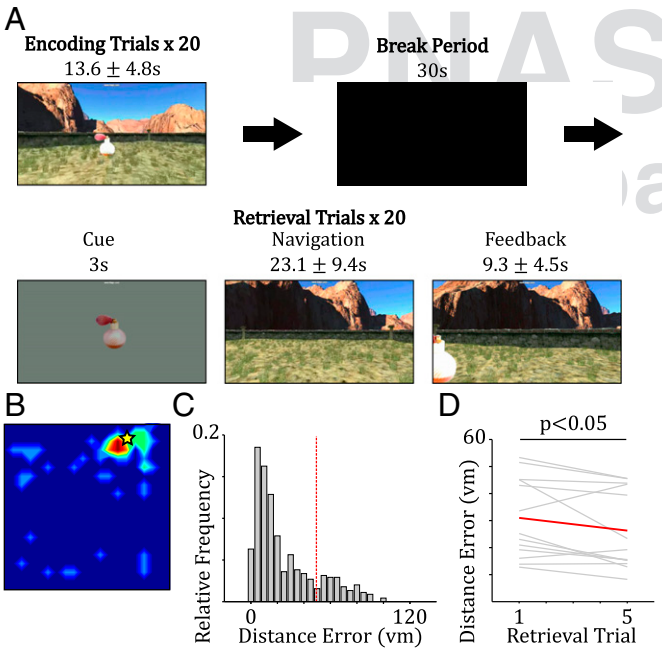

Fig. 1. Behavioral data. (*A*) Schematic of the spatial memory task. Participants navigate freely in a square VR environment, 100 vm per side, with distal cues for orientation. Participants memorize the location of one of four objects across 20 encoding trials (five for each object). Encoding is followed by a 30-s break period during which participants are instructed to focus on memorizing object locations. Each of 20 retrieval trials (five for each object) begins with a 3-s cue period, during which an image of one object is presented on screen. Participants are then placed back at one of four starting locations and are instructed to navigate to the remembered location of that object and make a response. Following this response, the object appears in its correct location to provide feedback on their performance in each trial. (*B*) Heat map of all responses for the object location in session one with the largest mean error across patients. The true object location is marked with a yellow star. (*C*) Histogram of Δds across all objects and patients. Chance performance is marked with a red dashed line. (*D*) Change in mean Δd for all objects across retrieval trials. Linear fits to each patient's performance are marked with a light gray line, and the average is marked with a thick red line.

Increased Hippocampal Theta Power Around Movement Onset. In the rodent hippocampal formation, significant increases in theta power have been observed during the stationary period immediately before movement onset (1, 2, 22–26). To establish whether similar increases in theta power could be observed in the human hippocampus, we focused our analysis on a 1-s period centered on movement onset that includes both the initial period of acceleration and an immediately preceding stationary interval (*Materials and Methods*). We began by comparing low-frequency oscillatory power on hippocampal electrode contacts during these movement-onset periods with periods of complete immobility across encoding and retrieval phases [excluding all trials that contained interictal spike (IIS) artifacts; see Table S3 for trial counts]. The resultant power spectrum exhibits two peaks centered around ~3.5 Hz and 7 Hz, respectively (Fig. 2 *A* and *B*), consistent with previous human intracranial studies that have described distinct task-related changes in separate low- and high-frequency theta bands (17–20). No significant event-related potentials (ERPs) were observed around movement onset, suggesting that these power increases reflect induced oscillations (Fig. S1). In addition, a comparison of power spectra for the remainder-of-movement and stationary periods also revealed peaks in the low- and high-frequency theta bands (Fig. 2*C*; see Fig. S2 for separate power spectra from each condition).

To further characterize these changes, we extracted mean z-scored power values from 3-Hz windows around the observed peaks in the low- and high-frequency theta band (i.e., 2–5 Hz and 6–9 Hz, respectively) for all movement periods. A repeated-measures ANOVA with levels of frequency band (low- versus high-frequency theta band), task phase (encoding versus retrieval), and movement period (movement onset versus remainder of movement versus stationary) revealed a main effect of movement period on hippocampal theta power [$F(2,16) = 10.1$, $P = 0.001$, $\eta_p^2 = 0.56$] but no effect of frequency band or task phase and no interactions (all $P > 0.17$) (Fig. 2*D*). Subsequent analyses indicated that this arose from an increase in theta power during movement-onset compared with stationary periods [$t(8) = 4.78$, $P < 0.005$, d = 1.59], consistent with previous rodent studies and our prior hypothesis (2, 26). We also note a trend toward greater theta power during movement-onset compared with remainder-of-movement periods [$t(8) = 2.16$, $P = 0.06$, $d = 0.72$] and during remainder-of-movement compared with stationary periods [$t(8) = 2.24$, $P = 0.06$, $d = 0.75$], although neither of these contrasts reached statistical significance. Moreover, z-scored theta power was greater than zero (i.e., from mean power in that frequency band across the entire recording, including task and nontask periods) during both movement-onset [$t(8) = 3.56$, $P < 0.01$, $d = 1.19$] and remainder-of-movement [$t(8) = 2.51$, $P < 0.05$, $d = 0.84$] but not during stationary [$t(8) = -0.33$, $P = 0.75$, $d = 0.11$] periods. Subsequent analysis indicated that these findings were not affected by differences in clinical characteristics among the patient population (*Supporting Information*).

These results demonstrate that a large but transient increase in both low and high human hippocampal theta power accompanies the onset of movement in a VR environment, analogous to the increase in rodent hippocampal theta power immediately before the onset of physical movement (1, 2, 22–26). Importantly, this effect may have been overlooked by previous paradigms that

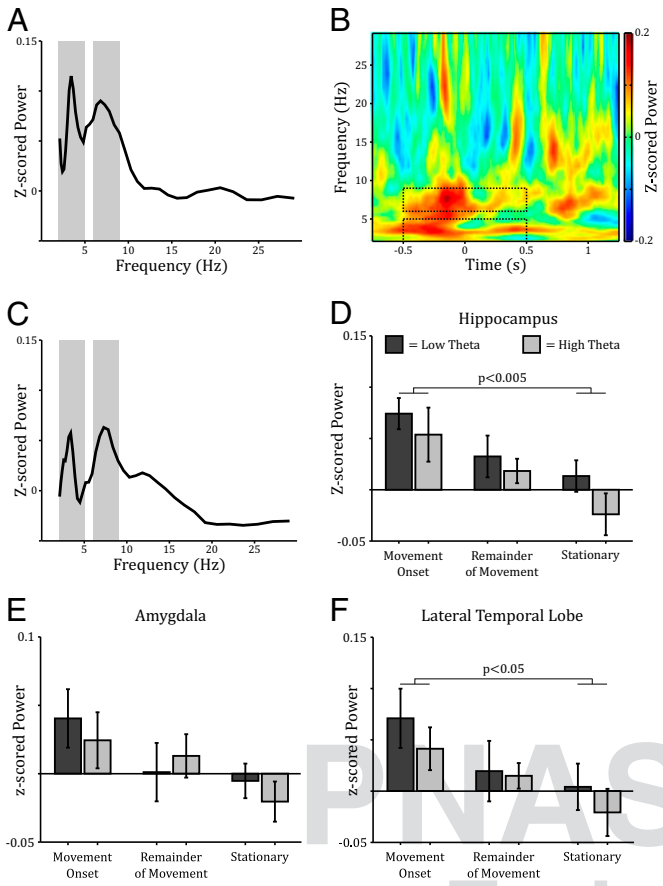

Fig. 2. Theta power changes during virtual movement across the temporal lobe. (*A*) Average power spectrum for movement-onset periods, baseline corrected by mean power at each frequency during stationary periods, for electrode contacts in the hippocampus. Power is increased in both low (2–5 Hz) and high (6–9 Hz) theta bands (marked in gray). (*B*) Spectrogram of power around virtual movement onset, baseline corrected by mean power at each frequency during stationary periods, for electrode contacts in the hippocampus. Black dashed regions indicate the low- and high-frequency theta bands for the 1-s period around movement onset. (*C*) Average power spectrum for remainder of movement periods, baseline corrected by mean power at each frequency during stationary periods, for electrode contacts in the hippocampus. Peaks in the low- and high-frequency theta bands (marked in gray) are visible but are less pronounced than during movement onset. (*D–F*) Mean z-scored power in the low (2–5 Hz) and high (6–9 Hz) theta bands during movement-onset, remainder-of-movement, and stationary periods in the hippocampus (*D*), amygdala (*E*), and lateral temporal lobe (*F*). Both low and high theta power are significantly increased during virtual movement onset, compared with stationary periods, on electrode contacts in the hippocampus and lateral temporal lobe but not on those located in the amygdala. In addition, mean z-scored power in the low- and high-frequency theta bands is greater than zero during movement onset on electrode contacts in the hippocampus and lateral temporal lobe and during the remainder of movement on electrode contacts in the hippocampus.

have compared "pure" movement and stationary periods (10–12, 14). Although theta power is strongest around movement onset, it does not differ statistically from the remainder of movement ($P < 0.06$) and remains elevated above baseline levels throughout both periods. Additional analyses indicate that theta power increases are specific to translational movements, as no analogous changes in low-frequency power are observed during the onset or remainder of purely rotational movement (Fig. S3). Interestingly, we also found no evidence for a difference in the magnitude of theta power increases around movement onset between encoding and retrieval periods. These findings are consistent with sensor-level MEG recordings using a similar paradigm (27) and suggest that the hippocampus may be one source of that observed signal, although other potential sources cannot be ruled out.

Increased Theta Power in the Lateral Temporal Lobe Around Movement Onset. Next, we asked whether movement-related theta oscillations were restricted to hippocampal electrode contacts or were also present in other temporal lobe regions. In rodents, theta has been observed in the amygdala during emotional arousal (30, 31) and in pre- and infralimbic cortices during spatial memory tasks (32, 33). In humans, theta oscillations appear to be widespread across the neocortex during navigation in VR environments (10, 11, 14) as well as during short- and long-term memory tasks (28, 34, 35). We therefore analyzed changes in z-scored theta power between movement periods across patients with depth electrode contacts located in the amygdala ($n = 12$ patients) and lateral temporal lobe ($n = 12$ patients; for complementary analysis of $n = 8$ patients with electrode contacts in all three regions, see *Supporting Information*).

For electrode contacts located in the amygdala, we note a trend toward a main effect of movement period [$F(2,22) = 3.09$, $P = 0.07$, $\eta_p^2 = 0.22$] but no other main effects or interactions (Fig. 2*E*; see Table S4 for trial counts). In addition, mean z-scored power values across both task phases and frequency bands were not different from zero during any movement period (all $P > 0.09$). Electrode contacts located in the lateral temporal lobe showed a main effect of movement period [$F(2,22) = 3.77$, $P < 0.05$, $\eta_p^2 = 0.26$] but no other main effects or interactions (all $P > 0.19$) (see Fig. 2*F* and Table S5 for trial counts). Subsequent analyses demonstrated that, as in the hippocampus, this arose from an increase in theta power during movement-onset periods compared with stationary periods [$t(11) = 2.35$, $P < 0.05$, $d = 0.68$], while there was no difference in theta power between movement-onset and remainder-of-movement periods [$t(11) = 1.74$, $P = 0.11$, $d = 0.50$] or between remainder-of-movement and stationary periods [$t(11) = 1.24$, $P = 0.24$, $d = 0.36$]. Moreover, mean z-scored theta power was greater than zero during movement-onset [$t(11) = 2.48$, $P < 0.05$, $d = 0.72$] but not during remainder-of-movement or stationary periods (both $P > 0.27$). Again, these findings were not affected by differences in clinical criteria among the patient population (*Supporting Information*).

These results demonstrate that changes in movement-related theta power within the amygdala and lateral temporal lobe show the same general pattern as those in the hippocampus, although these differences reach significance only on lateral temporal lobe electrode contacts. In light of this, we asked whether theta oscillations recorded on medial and lateral electrode contacts were the product of independent sources or a single theta generator. To answer this question, we examined the phase offset between theta band oscillations on all pairs of electrode contacts in the hippocampus and lateral temporal lobe during movement-onset periods. We found that the distribution of phase lags across patients was unimodal with zero mean in both the low (circular $V = 8.30$, $P < 0.001$) and high (circular $V = 8.89$, $P < 0.001$) theta bands. Similarly, distributions of trial-by-trial phase lags across all electrode pairs in the low- and high-frequency theta band for each individual patient were also unimodal with zero mean (all circular $V > 54.1$, all $P < 0.001$). Next, we examined the relationship between trial-by-trial variations in power within each region during movement-onset periods. We found that trial-by-trial power in the hippocampus and lateral temporal lobe were highly correlated in both the low [$t(8) = 10.36$, $P < 0.001$, $d = 3.45$] and high [$t(8) = 8.05$, $P < 0.001$, $d = 2.68$] theta bands. Each of these results is consistent with the influence of a single theta generator on both regions. Further analyses indicated that theta oscillations recorded on lateral temporal lobe contacts were

unlikely to arise as a result of volume conduction from the hippocampus (*Supporting Information*) (36). Hence, it appears that theta oscillations across the temporal lobe are actively driven by a single source. Although these data are insufficient to determine the location of that source, we note that theta synchrony across the hippocampal formation in rodents is thought to be driven by common input from the medial septum (26).

Movement-Related Theta Power Is Greater During Longer Paths. Having established that movement-onset and, to a lesser extent, remainder-of-movement periods were accompanied by a transient increase in theta power across the hippocampus and lateral temporal lobe, we asked whether theta amplitude during these periods had any behavioral correlates. Previous human intracranial EEG studies have demonstrated that theta power correlates with movement speed (13) and is greater when navigating more complex trajectories (15, 37). In our task, movement in the virtual environment accelerated quickly to a fixed top speed. However, we were able to examine whether theta power varied with distance traveled during each translational movement by separating movement-onset and remainder-of-movement periods for each patient according to whether the distance traveled was longer or shorter than their median path length.

In the hippocampus, a repeated-measures ANOVA with levels of frequency band (low- versus high-frequency theta band), movement period (movement onset versus remainder of movement), and path length (long versus short) showed a main effect of path length on theta power [$F(1,8) = 8.28$, $P < 0.05$, $\eta_p^2 = 0.51$] in addition to the expected main effect of movement period described above [$F(1,8) = 9.63$, $P < 0.05$, $\eta_p^2 = 0.55$] but no other main effects or interactions (all $P > 0.65$). Subsequent analyses demonstrated that this resulted from higher theta power both before and during longer paths [$t(8) = 2.88$, $P < 0.05$, $d = 0.96$] (Fig. 3 *A* and *B*). Importantly, z-scored power was also greater than zero both before and during long [$t(8) = 4.12$, $P < 0.005$, $d = 1.37$] but not short [$t(8) = 0.77$, $P = 0.46$, $d = 0.26$] paths.

Data from lateral temporal lobe contacts revealed similar results: a significant main effect of path length [$F(1,11) = 29.37$, $P < 0.001$, $\eta_p^2 = 0.73$] but no other main effects or interactions (all $P > 0.06$), which resulted from increased theta power before and during long, compared with short, paths [$t(11) = 5.42$, $P < 0.001$, $d = 1.56$] (Fig. 3 *C* and *D*), with z-scored theta power being greater than zero before and during long [$t(11) = 4.32$, $P < 0.005$, $d = 1.18$] but not short [$t(11) = 1.34$, $P = 0.22$, $d = 0.20$] paths (for complementary analysis of eight patients with electrode contacts in all regions, see *Supporting Information*). In both cases, we note that changes in movement-related oscillatory power between short and long paths were not restricted to the low- and high-frequency theta band but could be observed across a broad range of frequencies (<30 Hz) (Fig. 3 *B* and *D*). While this may be partly accounted for by spectral leakage from peaks in the low- and high-frequency theta band, the modulation of oscillatory power in other frequency bands might be addressed by future studies. Again, these results were generally unaffected by differences in clinical characteristics among the patient population (*Supporting Information*). In addition, we found no evidence for differences in movement-related theta power according to the duration of the stationary period preceding movement, when spatial orienting may occur, or between trials with high and low performance on electrode contacts in any region (all $P > 0.12$) (*Supporting Information*).

Hence, theta power increases across the temporal lobe during both movement-onset and remainder-of-movement periods are most pronounced for longer paths across the virtual environment but do not appear to covary with task performance. These results are consistent with movement-related theta oscillations mediating spatial processing rather than necessarily determining memory performance during encoding or retrieval: Theta power is increased immediately before and throughout translational movements, and the magnitude of that power increase indicates the distance traveled. Moreover, these findings implicate theta oscillations in spatial updating during both the planning and execution of translational movements (2).

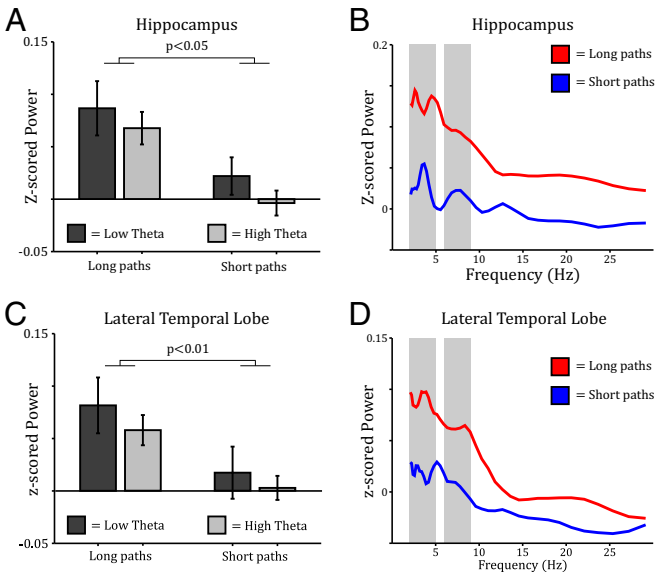

Fig. 3. Theta power changes with path length in the hippocampus and lateral temporal lobe. (*A* and *C*) Mean z-scored power in the low (2–5 Hz) and high (6–9 Hz) theta bands averaged across movement-onset and remainder-of-movement periods for long and short paths across the virtual environment on hippocampal (*A*) and lateral temporal lobe (*C*) electrode contacts. In each region, both low and high theta power are significantly increased during long paths compared with short paths. (*B* and *D*) Power spectra averaged across movement-onset and remainder-of-movement periods for long and short paths across the virtual environment in the hippocampus (*B*) and lateral temporal lobe (*D*). In both regions, broadband low-frequency oscillatory power is increased during long paths compared with short paths. Low (2–5 Hz) and high (6–9 Hz) theta bands are marked in gray.

Discussion

We have demonstrated that both low and high theta power in the human hippocampus and lateral temporal lobe are increased around movement onset in a virtual environment, compared with stationary periods. These theta power increases appear to peak during the stationary interval immediately before movement onset (Fig. 2*B*), although our movement-onset periods also incorporate an initial period of acceleration that may contribute to the observed effect. Analogous results have been obtained from the rodent hippocampus, in which theta power increases are seen immediately before the onset of translational movement in both the LFP (1, 2, 23–26) and in the membrane potential of single neurons (22). Hence, this finding strengthens the translational connection between studies of movement-related theta in human and rodent models. Importantly, this increase in theta power around movement onset may have been overlooked by previous human intracranial recording studies that have exclusively compared pure movement and stationary periods that tend to be of short duration (10–12, 14). Theta power increases are not specific to movement-onset periods, however: Both low and high theta power remained above baseline levels during the remainder of movement in the hippocampus and, to a lesser extent, in the lateral temporal lobe. These data are consistent with the rodent literature and several previous intracranial studies that have described an increased prevalence of theta band

oscillations in both the hippocampus and neocortex during movement compared with stationary periods (10–12).

In addition, we have shown that movement-related power increases in low- and high-frequency theta bands are greater both before and during longer paths, but in neither band does power appear to correlate significantly with task performance or vary between periods of encoding and retrieval. These results suggest a role for theta oscillations in both the planning and execution of translational movements during an ethologically valid navigation task. This is consistent with several previous studies showing that theta oscillations are more prevalent during complex spatial navigation tasks (i.e., long versus short mazes) (15, 37), faster translational movements (13), and virtual teleportation over longer versus shorter distances in the absence of visual or self-motion cues (38). Importantly, this study also extends those results by focusing on changes in theta power, which can be more easily related to rodent data than the prevalence of theta oscillations, by examining active self-directed movements, which have greater ethological validity than periods of passive movement or teleportation, and by showing increased theta power before the onset of longer paths, supporting the hypothesis that theta oscillations are involved in spatial updating during the planning, as well as the execution, of translational movements (2).

Previous studies have highlighted two important differences between rodent and human movement-related theta oscillations (20). First, human theta oscillations appear in transient bursts that typically last several cycles, in contrast to the continuous rhythm in the rodent hippocampus (15, 16), and it is not clear whether these sporadic oscillations could encode continuous self-motion information (8, 20). However, it is possible that location estimates are updated intermittently during theta bursts, in accordance with the outcome of planned movements, rather than tracked continually throughout movement by an ongoing theta oscillation. Such a mechanism would be consistent with our observation that theta power was greater before movement onset and for longer translational movements. Alternatively, estimates of current location might be intermittently updated by tracking the relative location of visual landmarks during theta bursts, and distance traveled might be estimated by tracking the temporal duration of each translational movement. Further investigations using experimental paradigms that can dissociate the relative influence of temporal duration and visual input on estimates of distance traveled are required to address this issue (38).

Second, human movement-related theta oscillations apparently exist in two different frequency bands, one lower and closer to the traditional delta band and one higher and closer to the frequency of rodent hippocampal theta (10, 13, 20). It has been suggested that low theta may be the analog of rodent hippocampal theta, as it shows more prominent subsequent memory effects (17, 18); phase coupling with rhinal cortices (39); and modulates the firing rate of hippocampal cells during virtual navigation (40). Two distinct hippocampal theta oscillations have also been identified in rodents: type 1, which is typically modulated by translational movement and has a higher frequency, and type 2, which is typically modulated by anxiety and arousal and has a lower frequency, although still clearly above the delta band (41). However, the fact that both low and high theta power appear to be modulated by translational movement in our data, while no manipulations of anxiety or arousal were made, suggests that both correspond to rodent type 1 theta. In fact, we found no evidence for a functional distinction between low and high theta oscillations during any movement period, suggesting that these frequency bands might coexist to mediate human spatial processing. It is also possible that low and high theta do not reflect independent processes but instead are a single oscillation that varies dynamically over a broad frequency range (42, 43). This could explain the presence of spike-LFP phase coupling in single neurons within the human hippocampal formation in the absence of a strong fixed frequency baseline oscillation (40). Interestingly, the zero phase lag observed here between theta oscillations on hippocampal and lateral temporal lobe electrode contacts contrasts with previous reports of stable nonzero phase differences between theta oscillations in these regions during a nonspatial memory task (19). This might be accounted for by mnemonic function preferentially recruiting type 2 theta oscillations that are independently generated by separate hippocampal and cortical sources.

Three important caveats to the results presented here merit further discussion. First, contrasts between movement and stationary periods are confounded by the fact that patients must press a button to move across the VR environment but not to remain stationary. This raises the possibility that observed changes in theta power result from button pressing rather than from translational movement per se. However, our data show that button pressing in the absence of translational movement is not associated with changes in either low or high theta power (Fig. S4 and accompanying text), consistent with several previous studies showing no correlation between button pressing and theta power in the human hippocampus or neocortex (10, 11, 34, 36). Second, it is important to emphasize that patients do not physically locomote during the task. In rodents, both movement-related theta oscillations and the spatial modulation of neural firing patterns are weaker during passive movement through an environment (44, 45). Similarly, although LFP theta oscillations appear normal in rodent VR recordings (22, 46), the relationship between running speed and theta frequency is reduced (47). Hence, it is possible that the power, duration, and spectral fingerprint of movement-related theta in humans may differ during physical locomotion. Interestingly, recent depth electrode recordings taken from the hippocampi of a small number of patients hint at an increased prevalence of high-frequency theta oscillations during real-world ambulation (12). Finally, all human intracranial EEG studies must address the issue of extrapolating findings in epilepsy patients to the wider population. Reassuringly, the results presented here qualitatively replicate findings from a previous MEG study of healthy participants performing a similar task (27). The increase in theta power around movement onset observed in that study could not be localized, but the data presented here suggest the hippocampus as one candidate, although other potential sources cannot be ruled out. Further investigation with more advanced MEG source-localization techniques might elucidate this issue (48).

In summary, we have shown that movement onset is associated with a pronounced increase in both low and high theta power in the human hippocampus that also persists during the remainder of movement. Importantly, movement-related theta power is also greater both before and during longer translational paths. These findings strengthen the link between rodent and human hippocampal theta oscillations and provide additional insight into the mechanisms of human spatial navigation.

Materials and Methods

Nineteen patients with pharmaco-resistant epilepsy completed a spatial memory task used in several previous neuroimaging studies (Fig. 1*A*) (21, 27, 28) in which they were asked to remember object locations in the absence of direct cues, similar to the Morris water maze (49). Three of these patients were excluded due to technical difficulties, one patient could not perform the task, and two patients failed to produce a sufficient number of stationary trials as they moved continuously in the VR environment. This left 13 patients: six female, 11 right-handed, with a mean age ± SD of 29.3 ± 7.8 y (see Tables S1 and S2 for further details). Four patients completed one session of the task, and nine patients completed two sessions. The second session made use of the same environment but used four new objects in new locations.

Surgery and subsequent intracranial recordings were carried out at the National Hospital for Neurology and Neurosurgery, London. All patients had platinum Spencer probe depth electrodes (Severn Healthcare Technologies) inserted into the medial temporal lobe: in the right hemisphere in eight

patients, in the left hemisphere in four patients, and one bilateral implantation. Electrode locations were determined solely by clinical criteria, ascertained by visual inspection of postimplantation CT and/or MRI scans by R.R. and a consultant neurophysiologist (B.D.), and verified by an fMRI expert (J.A.B.). The presence of hippocampal damage was assessed, when histopathology was not available, by structural MRI at 3T including quantification of hippocampal volumes and T2 relaxation times. The study was approved by the National Health Service research ethics committee, and all patients gave written informed consent. Patients were seizure free for at least 24 h before participation.

Depth EEG was recorded continuously at a sample rate of 1,024 Hz (patients 4 and 10) or 512 Hz (all other patients) using either a NicoletOne long-term monitoring system (Natus Medical, Inc.) (patients 1–6) or Micromed SD long-term monitoring system (Micromed) (patients 7–13). Recordings made at a higher sampling rate were down-sampled to 512 Hz, to match those from the majority of patients, before any analyses were performed. Recordings made using the Micromed system were also subject to a 0.02-Hz digital high-pass filter. For each patient, a postimplantation CT image showing the implanted electrodes was coregistered with, and then overlaid upon, a preimplantation T1-weighted MR image. Candidate reference electrodes were chosen from contacts located in white matter by visual inspection of the overlaid images. EEG recordings from each candidate reference electrode were then visually inspected, and a single contact with little or no apparent EEG activity was chosen as the reference for all subsequent recordings. Audio triggers produced by the VR laptop were recorded on the monitoring system, allowing the EEG to be aligned with movement and task information sampled at 25 Hz.

Further information can be found in *SI Materials and Methods*.

ACKNOWLEDGMENTS. We thank all patients who participated in this study and Mike Anderson, Helen Barron, Aidan Horner, Raphael Kaplan, Catherine Scott, and Ewa Zotow for useful discussions during the preparation of this manuscript. This work was supported by the Wellcome Trust, the UK Medical Research Council, the European Research Council, and the Department of Health's National Institute for Health Research University College London Hospitals/University College London Biomedical Research Centre.

1. Vanderwolf CH (1969) Hippocampal electrical activity and voluntary movement in the rat. *Electroencephalogr Clin Neurophysiol* 26:407–418.
2. O'Keefe J, Nadel L (1978) *The Hippocampus as a Cognitive Map* (Oxford Univ Press, Oxford, UK).
3. McFarland WL, Teitelbaum H, Hedges EK (1975) Relationship between hippocampal theta activity and running speed in the rat. *J Comp Physiol Psychol* 88:324–328.
4. Rivas J, Gaztelu JM, García-Austt E (1996) Changes in hippocampal cell discharge patterns and theta rhythm spectral properties as a function of walking velocity in the guinea pig. *Exp Brain Res* 108:113–118.
5. Sławińska U, Kasicki S (1998) The frequency of rat's hippocampal theta rhythm is related to the speed of locomotion. *Brain Res* 796:327–331.
6. Jeewajee A, Barry C, O'Keefe J, Burgess N (2008) Grid cells and theta as oscillatory interference: Electrophysiological data from freely moving rats. *Hippocampus* 18: 1175–1185.
7. Brandon MP, et al. (2011) Reduction of theta rhythm dissociates grid cell spatial periodicity from directional tuning. *Science* 332:595–599.
8. Burgess N, O'Keefe J (2011) Models of place and grid cell firing and theta rhythmicity. *Curr Opin Neurobiol* 21:734–744.
9. Koenig J, Linder AN, Leutgeb JK, Leutgeb S (2011) The spatial periodicity of grid cells is not sustained during reduced theta oscillations. *Science* 332:592–595.
10. Ekstrom AD, et al. (2005) Human hippocampal theta activity during virtual navigation. *Hippocampus* 15:881–889.
11. Jacobs J, et al. (2010) Right-lateralized brain oscillations in human spatial navigation. *J Cogn Neurosci* 22:824–836.
12. Bohbot VD, Copara MS, Gotman J, Ekstrom AD (2017) Low-frequency theta oscillations in the human hippocampus during real-world and virtual navigation. *Nat Commun* 8:14415.
13. Watrous AJ, Fried I, Ekstrom AD (2011) Behavioral correlates of human hippocampal delta and theta oscillations during navigation. *J Neurophysiol* 105:1747–1755.
14. Caplan JB, et al. (2003) Human theta oscillations related to sensorimotor integration and spatial learning. *J Neurosci* 23:4726–4736.
15. Kahana MJ, Sekuler R, Caplan JB, Kirschen M, Madsen JR (1999) Human theta oscillations exhibit task dependence during virtual maze navigation. *Nature* 399:781–784.
16. Watrous AJ, et al. (2013) A comparative study of human and rat hippocampal low-frequency oscillations during spatial navigation. *Hippocampus* 23:656–661.
17. Sederberg PB, et al. (2007) Hippocampal and neocortical gamma oscillations predict memory formation in humans. *Cereb Cortex* 17:1190–1196.
18. Fell J, et al. (2011) Medial temporal theta/alpha power enhancement precedes successful memory encoding: Evidence based on intracranial EEG. *J Neurosci* 31: 5392–5397.
19. Lega BC, Jacobs J, Kahana M (2012) Human hippocampal theta oscillations and the formation of episodic memories. *Hippocampus* 22:748–761.
20. Jacobs J (2013) Hippocampal theta oscillations are slower in humans than in rodents: Implications for models of spatial navigation and memory. *Philos Trans R Soc Lond B Biol Sci* 369:20130304.
21. Doeller CF, King JA, Burgess N (2008) Parallel striatal and hippocampal systems for landmarks and boundaries in spatial memory. *Proc Natl Acad Sci USA* 105:5915–5920.
22. Schmidt-Hieber C, Häusser M (2013) Cellular mechanisms of spatial navigation in the medial entorhinal cortex. *Nat Neurosci* 16:325–331.
23. Green JD, Arduini AA (1954) Hippocampal electrical activity in arousal. *J Neurophysiol* 17:533–557.
24. Whishaw IQ, Vanderwolf CH (1973) Hippocampal EEG and behavior: Changes in amplitude and frequency of RSA (theta rhythm) associated with spontaneous and learned movement patterns in rats and cats. *Behav Biol* 8:461–484.
25. Bland BH, et al. (2006) Amplitude, frequency, and phase analysis of hippocampal theta during sensorimotor processing in a jump avoidance task. *Hippocampus* 16: 673–681.
26. Fuhrmann F, et al. (2015) Locomotion, theta oscillations, and the speed-correlated firing of hippocampal neurons are controlled by a medial septal glutamatergic circuit. *Neuron* 86:1253–1264.
27. Kaplan R, et al. (2012) Movement-related theta rhythm in humans: Coordinating self-directed hippocampal learning. *PLoS Biol* 10:e1001267.
28. Kaplan R, et al. (2014) Medial prefrontal theta phase coupling during spatial memory retrieval. *Hippocampus* 24:656–665.
29. Spiers HJ, et al. (2001) Unilateral temporal lobectomy patients show lateralized topographical and episodic memory deficits in a virtual town. *Brain* 124:2476–2489.
30. Seidenbecher T, Laxmi TR, Stork O, Pape HC (2003) Amygdalar and hippocampal theta rhythm synchronization during fear memory retrieval. *Science* 301:846–850.
31. Paré D, Collins DR, Pelletier JG (2002) Amygdala oscillations and the consolidation of emotional memories. *Trends Cogn Sci* 6:306–314.
32. Young CK, McNaughton N (2009) Coupling of theta oscillations between anterior and posterior midline cortex and with the hippocampus in freely behaving rats. *Cereb Cortex* 19:24–40.
33. Benchenane K, et al. (2010) Coherent theta oscillations and reorganization of spike timing in the hippocampal- prefrontal network upon learning. *Neuron* 66:921–936.
34. Raghavachari S, et al. (2001) Gating of human theta oscillations by a working memory task. *J Neurosci* 21:3175–3183.
35. Sederberg PB, Kahana MJ, Howard MW, Donner EJ, Madsen JR (2003) Theta and gamma oscillations during encoding predict subsequent recall. *J Neurosci* 23: 10809–10814.
36. Sirota A, et al. (2008) Entrainment of neocortical neurons and gamma oscillations by the hippocampal theta rhythm. *Neuron* 60:683–697.
37. Caplan JB, Madsen JR, Raghavachari S, Kahana MJ (2001) Distinct patterns of brain oscillations underlie two basic parameters of human maze learning. *J Neurophysiol* 86:368–380.
38. Vass LK, et al. (2016) Oscillations go the distance: Low-frequency human hippocampal oscillations code spatial distance in the absence of sensory cues during teleportation. *Neuron* 89:1180–1186.
39. Fell J, et al. (2003) Rhinal-hippocampal theta coherence during declarative memory formation: Interaction with gamma synchronization? *Eur J Neurosci* 17:1082–1088.
40. Jacobs J, Kahana MJ, Ekstrom AD, Fried I (2007) Brain oscillations control timing of single-neuron activity in humans. *J Neurosci* 27:3839–3844.
41. Kramis R, Vanderwolf CH, Bland BH (1975) Two types of hippocampal rhythmical slow activity in both the rabbit and the rat: Relations to behavior and effects of atropine, diethyl ether, urethane, and pentobarbital. *Exp Neurol* 49:58–85.
42. Cohen MX (2014) Fluctuations in oscillation frequency control spike timing and coordinate neural networks. *J Neurosci* 34:8988–8998.
43. Orchard J (2015) Oscillator-interference models of path integration do not require theta oscillations. *Neural Comput* 27:548–560.
44. Terrazas A, et al. (2005) Self-motion and the hippocampal spatial metric. *J Neurosci* 25:8085–8096.
45. Winter SS, Mehlman ML, Clark BJ, Taube JS (2015) Passive transport disrupts grid signals in the parahippocampal cortex. *Curr Biol* 25:2493–2502.
46. Harvey CD, Collman F, Dombeck DA, Tank DW (2009) Intracellular dynamics of hippocampal place cells during virtual navigation. *Nature* 461:941–946.
47. Ravassard P, et al. (2013) Multisensory control of hippocampal spatiotemporal selectivity. *Science* 340:1342–1346.
48. Meyer SS, et al. (2017) Using generative models to make probabilistic statements about hippocampal engagement in MEG. *Neuroimage* 149:468–482.
49. Morris RGM, Garrud P, Rawlins JNP, O'Keefe J (1982) Place navigation impaired in rats with hippocampal lesions. *Nature* 297:681–683.
50. Lachaux J-P, Rodriguez E, Martinerie J, Varela FJ (1999) Measuring phase synchrony in brain signals. *Hum Brain Mapp* 8:194–208.
51. Berens P (2009) CircStat: A Matlab toolbox for circular statistics. *J Stat Softw* 31:1–21.

Supporting Information

Bush et al. 10.1073/pnas.1708716114

SI Materials and Methods

Patient Population. Nineteen patients with pharmaco-resistant epilepsy were recruited. Three of these patients were excluded due to technical difficulties, one patient could not perform the task, and two patients failed to produce a sufficient number of stationary trials as they moved continuously in the VR environment. This left 13 patients: six female, 11 right-handed, with a mean age ± SD of 29.3 ± 7.8 y (see Tables S1 and S2 for further details). Surgery and subsequent intracranial recordings were carried out at the National Hospital for Neurology and Neurosurgery, London. All patients had platinum Spencer probe depth electrodes (Severn Healthcare Technologies) inserted into the medial temporal lobe: in the right hemisphere in eight patients, in the left hemisphere in four patients, and one bilateral implantation. Electrode locations were determined solely by clinical criteria, confirmed by visual inspection of postimplantation CT and/or MRI scans by R.R. and a consultant neurophysiologist (B.D.), and verified by an fMRI expert (J.A.B.). The presence of hippocampal damage was assessed, when histopathology was not available, by structural MRI at 3T including quantification of hippocampal volumes and T2 relaxation times. The study was approved by the National Health Service research ethics committee, and all patients gave written informed consent. Patients were seizure free for at least 24 h before participation.

Task. Patients completed a spatial memory task used in several previous neuroimaging studies (Fig. 1*A*) (21, 27, 28) in which they were asked to remember object locations in the absence of direct cues, similar to the Morris water maze (49). Participants navigate freely in a square VR environment, 100 vm per side, which is projected onto a laptop screen placed in front of them. Movement within the VR environment is controlled using arrow keys on the laptop keyboard, with virtual movement accelerating quickly to a fixed top speed. Distal cues surround the environment to orient the participant.

During each encoding trial, participants are asked to navigate toward and encode the location of one of four different objects. Only one object is visible in each encoding trial, and there are five encoding trials for each of the four objects, giving a total of 20 encoding trials in each session. Object locations are constant across encoding trials. Following encoding, participants are given a 30-s break during which they are instructed to focus on memorizing the object locations. After the break period, each retrieval trial begins with a 3-s cue period during which an image of one object is displayed on a plain gray background. Participants are subsequently placed back in the virtual environment at one of four randomly selected starting locations and orientations and are asked to navigate to the remembered location of that object and make a response. Once participants have made a response, the object appears in its correct location to provide feedback on their performance, and the trial ends when participants navigate to the true location of the visible object. There are five retrieval trials for each object, giving a total of 20 retrieval trials in each session.

Four patients completed one session of the task, and nine patients completed two sessions. The second session made use of the same environment but used four new objects in new locations. The distance error Δd for each trial is defined as the absolute distance between the location at which the response was made and the true location of that object. Chance performance was calculated as the mean distance between the location of each object and every other location in the environment (i.e., by treating every location in the environment as an equally likely response location). Changes in Δd across retrieval trials were assessed by first performing linear regression on the Δd in each trial against the retrieval trial number for that object, averaging those regression coefficients across objects for each patient, and performing a one-sampled t test on mean regression coefficients across patients.

Intracranial EEG Recordings and Artifact Detection. Depth EEG was recorded continuously at a sample rate of 1,024 Hz (patients 4 and 10) or 512 Hz (all other patients) using either a Nicolet NicoletOne long-term monitoring system (Natus Medical, Inc.) (patients 1–6) or a Micromed SD long-term monitoring system (Micromed) (patients 7–13). Recordings made at a higher sampling rate were down-sampled to 512 Hz, to match those from the majority of patients, before any analyses were performed. Recordings made using the Micromed system were also subject to a 0.02-Hz digital high-pass filter. For each patient, a postimplantation CT image showing the implanted electrodes was coregistered with, and then overlaid upon, a preimplantation T1-weighted MR image. Candidate reference electrodes were chosen from contacts located in white matter by visual inspection of the overlaid images. EEG recordings from each candidate reference electrode were then visually inspected, and a single contact with little or no apparent EEG activity was chosen as the reference for all subsequent recordings.

Audio triggers produced by the VR laptop were recorded on the monitoring system, allowing the EEG to be aligned with movement and task information sampled at 25 Hz. We analyze recordings from electrode contacts in three regions of interest: the hippocampus (nine patients with mean ± SD of 4.8 ± 1.6 contacts; range, 2–8 contacts), amygdala (12 patients with 2.7 ± 0.7 contacts; range, 2–4 contacts), and lateral temporal lobe (12 patients with 7.3 ± 3.0 contacts; range, 2–12 contacts) (see Table S1 for further details). These recordings, which included all experimental sessions performed by each patient as well as several minutes of EEG from before and after those sessions, were first inspected for interictal spike (IIS) events and other artifacts by a trained epileptologist (S.G.) and verified independently by an EEG analysis expert (D.B.). The timing of all IIS and other artifacts on each channel were recorded and stored for subsequent analyses. All analyses were carried out using custom Matlab (MathWorks) scripts.

Epochs of Interest. Analysis of EEG recordings focused on three main periods of interest: movement-onset, remainder-of-movement, and stationary periods. Movement-onset epochs were defined as −0.5:0.5-s windows around the onset of periods of continuous translational movement in the virtual environment that lasted >1 s and were preceded by periods of complete immobility (i.e., an absence of either translational or rotational movement) that lasted >0.5 s. This was motivated by three factors: that the time window be centered on movement onset, to incorporate both the initial period of acceleration and an immediately preceding stationary period associated with prominent theta power increases in the rodent hippocampus (1, 2, 22–26); that the window be of sufficient duration to assay changes in low-frequency power (i.e., ≥1 s, to incorporate two or more cycles of an oscillation at ≥2 Hz); and that the time window be short enough to provide a sufficient number of remainder-of-movement trials of at least the same duration (i.e., ≤1 s, given that the average movement duration across patients was ∼2 s; see Tables S3–S5).

Remainder-of-movement epochs were defined as >1-s time windows of continuous translational movement within the virtual

environment that lasted >1.5 s, beginning 0.5 s after the onset of movement and ending when movement ceased. Stationary epochs were defined as >1-s time windows of complete immobility within the virtual environment that lasted >1.5 s, beginning immediately after the cessation of movement and ending 0.5 s before the onset of subsequent movement (see Tables S3–S5 for trial counts and movement epoch lengths for all patients).

ERP Analysis. ERPs for each epoch of interest were obtained by extracting raw EEG signals for each trial, subtracting the mean amplitude across that trial, and then z-scoring using the mean and SD of signal amplitude across the entire recording on each channel. EEG signals from all artifact-free trials during the same epoch were then averaged to generate the ERP for that epoch. To identify any significant ERPs, we performed one-sample *t* tests at each time point with a more stringent threshold of $P < 0.001$ to compensate for multiple comparisons across 1,024 time points. Significant ERPs were subsequently defined as any set of at least 25 contiguous time points (i.e., ≥50 ms period) that exceeded this threshold.

Time–Frequency Analysis. Estimates of dynamic oscillatory power during periods of interest were obtained by convolving the EEG signal with a five-cycle Morlet wavelet and squaring the absolute value of the convolved signal. The wavelet transform was preferred to the Fourier transform as it does not assume stationarity in EEG recordings. Power values were obtained for 39 logarithmically spaced frequency bands in the 2–30 Hz range. Time–frequency data were extracted from 1 s before the start of each period of interest to 1 s after the end of that period, and data from those 1-s epochs before and after the period of interest were discarded after convolution to avoid edge effects. All trials that included IIS or other artifacts, either within the period of interest or during the 1-s padding windows, were excluded from all analyses presented here (see Tables S3–S5 for trial counts). All power values were log transformed, and power values from each electrode for each condition were then z-scored using the mean and SD of log-transformed power values in each frequency band during artifact-free periods throughout the entire EEG recording.

To generate power spectra, the mean of dynamic oscillatory power estimates or differences in oscillatory power between conditions was taken over the time window of interest. To perform baseline correction on time–frequency data for display purposes (i.e., Fig. 2 *A*–*C*), log-transformed power values were averaged across stationary periods for each frequency band, and those average values were subtracted from the log-transformed power values at each time point in the movement-onset or remainder-of-movement data. To examine changes in oscillatory power within specific frequency bands and assess correlations among oscillatory power, task performance, and IIS events in each trial, dynamic estimates of log-transformed oscillatory power were averaged over the time and frequency windows of interest. Mean power values were then averaged across all electrode contacts in each cortical region to provide a single value for each patient. Changes in oscillatory power according to task demands were analyzed using repeated-measures ANOVAs and post hoc one-sample *t* tests with Bonferroni correction for multiple comparisons where appropriate.

Phase Coupling Analysis. To estimate the phase offset between simultaneous theta band oscillations on pairs of electrode contacts, the signal from each region, including a 1-s window both before the start and after the end of each epoch, was band-pass filtered in the frequency range of interest (i.e., 2–5 Hz or 6–9 Hz) using a zero phase, 400th order finite impulse response (FIR) filter. The phase difference between all pairs of electrode contacts between regions at each time point was then extracted. Phase coupling was estimated using the phase-locking value, which is equal to the resultant vector length of the phase difference distribution across the time window of interest (50). Finally, the circular mean phase difference between filtered signals from each pair of electrode contacts within each epoch was computed, and then the circular mean value across all pairs of electrode contacts from each patient was entered into a second-level circular V test using the Toolbox for Circular Statistics in Matlab (51) to assess whether the distribution of phase differences across patients was drawn from a unimodal distribution with zero mean.

SI Results

ERPs at Virtual Movement Onset. It is important to ascertain whether the observed increase in theta power around the onset of movement in the VR environment results from induced or evoked oscillations. In the latter case, one might expect to observe a simultaneous ERP. Hence, we examined EEG recordings from each cortical region at movement onset for any evidence of ERPs. However, we found no significant time-locked deflections in EEG recordings from the hippocampus (Fig. S1 *A* and *B*), amygdala (Fig. S1 *C* and *D*), or lateral temporal lobe (Fig. S1 *E* and *F*) that might explain the observed increase in theta power shown in Fig. 2. Hence, we conclude that these power changes reflect induced, rather than evoked, oscillations.

Raw Power Spectra for Each Movement Condition Across Temporal Lobe Recording Sites. To ascertain whether peaks were present in the low and high theta band during each movement condition separately, or whether such peaks were specific to movement-onset and remainder-of-movement periods, separate power spectra from each cortical region were generated for each movement condition (Fig. S2). These power spectra demonstrate that peaks in both the low and high theta band can be observed during movement-onset periods in all cortical regions, alongside a general increase in low-frequency (<10 Hz) oscillatory power above baseline levels (i.e., above the mean power in that frequency band across the whole recording). Conversely, during stationary periods, peaks are observed only in the low theta band, and low-frequency power is generally reduced compared with baseline levels.

Differences in Movement-Related Theta Power According to Clinical Criteria. Given that the EEG recordings examined here are taken from a clinical population, we wished to assess whether any of the main effects observed, that is, increased theta power during movement onset compared with stationary periods and increased theta power both before and during longer translational paths, were influenced by clinical characteristics. Between-subjects factors that might affect these results include the implanted hemisphere (language-dominant versus nondominant), the presence of hippocampal sclerosis, and the presence of a temporal lobe seizure onset zone (see Table S2 for further details). Hence, we compared the magnitude of theta power changes between groups of patients that differed according to these criteria using a series of independent sample *t* tests. In each case, we must note that the relatively small sample sizes used urge some caution when interpreting these findings.

First, we found no differences in the magnitude of theta power increases during movement onset, compared with stationary periods, on hippocampal electrode contacts between patients with depth electrodes implanted in the language-dominant versus nondominant hemisphere, in patients with or without hippocampal sclerosis, and in patients with or without a temporal seizure onset zone (all $P > 0.1$). Similarly, we found no differences in theta power increases during movement onset, compared with stationary periods, on either amygdala or lateral temporal lobe electrode contacts between patients with depth

electrodes implanted in the language-dominant versus non-dominant hemisphere, in patients with or without hippocampal sclerosis, and in patients with or without a temporal seizure onset zone (all $P > 0.28$).

Second, we found no evidence for differences in theta power during long versus short paths between patients with or without sclerotic hippocampi or between patients with or without a temporal seizure onset zone in any region (all $P > 0.21$). Interestingly, however, the observed theta power increases for long versus short paths did show a trend toward laterality on hippocampal electrode contacts, being greater in patients with electrodes implanted in the language-dominant hemisphere [$t(7) = 2.25$, $P = 0.06$, Cohen's $d = 0.80$]. Conversely, no such laterality was observed in either the amygdala or lateral temporal lobe (both $P > 0.13$).

Theta Power Changes Associated with Rotational Movement. To ascertain whether changes in theta power were specific to translational movement, we analyzed changes in low and high theta power during equivalent periods of purely rotational movement: 1-s rotation-onset epochs centered on the onset of purely rotational movements that lasted >1 s and were preceded by periods of complete immobility that lasted >0.5 s and >1-s remainder-of-rotation epochs beginning 0.5 s after the onset of continuous rotational movement within the virtual environment that lasted >1.5 s and ending when that movement ceased.

For electrode contacts in the hippocampus, a repeated-measures ANOVA with levels of theta band (low versus high) and rotation epoch (rotation onset versus remainder of rotation versus stationary) showed no main effects or interactions (all $P > 0.16$) (Fig. S3 *A–D*). However, we note a trend toward z-scored low theta power during rotation-onset periods being greater than zero [i.e., from the mean power in that frequency band across the entire recording; $t(8) = 2.29$, $P = 0.052$, $d = 0.76$, all other $P > 0.13$]. Similar results were obtained from electrode contacts in the amygdala, where no main effects or interactions were identified (all $P > 0.12$), and z-scored power was not greater than zero in any condition (all $P > 0.15$) (Fig. S3*E*), and in the lateral temporal lobe, where no main effects or interactions were identified (all $P > 0.14$), although we note a similar trend toward z-scored low theta power during rotation-onset periods being greater than zero [$t(8) = 2.20$, $P = 0.05$, $d = 0.64$; all other $P > 0.38$] (Fig. S3*F*). Overall, these results suggest that movement-related changes in theta power are specific to translational movements, as purely rotational movements do not significantly modulate theta power in any temporal lobe region.

Comparison of Theta Power Changes Across Temporal Lobe Recording Sites. To ascertain whether we could identify any systematic differences in z-scored theta power across temporal lobe recording sites during movement, we analyzed data from eight patients who had depth electrode contacts in all three cortical regions. A repeated-measures ANOVA with levels of theta band (low versus high), region (hippocampus versus amygdala versus lateral temporal lobe), and movement epoch (movement onset versus remainder of movement versus stationary) revealed a main effect of movement epoch [$F(2,14) = 11.58$, $P = 0.001$, $\eta_p^2 = 0.62$] but no other main effects or interactions (all $P > 0.34$). Subsequent analyses demonstrated that this results from an increase in theta power during movement-onset, compared with both the remainder-of-movement [$t(7) = 3.02$, $P < 0.05$, $d = 1.07$] and stationary [$t(7) = 5.47$, $P < 0.001$, $d = 1.93$] periods. Moreover, z-scored theta power was greater than zero during movement-onset periods [$t(7) = 4.79$, $P < 0.005$, $d = 1.70$] but not during remainder-of-movement or stationary periods (both $P > 0.17$).

Similarly, we characterized changes in theta power with path length across temporal lobe recording sites by analyzing data from the same eight patients. In addition to the expected main effect of movement [$F(1,7) = 18.57$, $P < 0.005$, $\eta_p^2 = 0.73$], a repeated-measures ANOVA with levels of theta band (low versus high), cortical region (hippocampus versus amygdala versus lateral temporal lobe), movement epoch (movement onset versus remainder of movement), and path length (long versus short) identified a main effect of path length [$F(1,7) = 5.81$, $P < 0.05$, $\eta_p^2 = 0.45$] and a region × path length interaction [$F(1,7) = 8.76$, $P < 0.005$, $\eta_p^2 = 0.56$; all others $P > 0.09$]. Subsequent analyses demonstrate that these effects were driven by increased theta power during longer paths [$t(7) = 2.41$, $P < 0.05$, $d = 0.85$] and a difference in theta power between the lateral temporal lobe and amygdala during long paths [$t(7) = 3.33$, $P < 0.05$, $d = 1.18$] with no difference between the hippocampus and amygdala or lateral temporal lobe (both $P > 0.1$). Hence, data from recordings across the temporal lobe in these eight patients generally show the same pattern of results described for hippocampal and lateral temporal lobe electrode contacts in the main text, with theta power elevated during movement onset and movement-related theta power being greater for longer translational paths.

Theta Oscillations in Lateral Temporal Lobe Do Not Reflect Volume Conduction from Hippocampus. Given that theta oscillations recorded on electrode contacts in the hippocampus and lateral temporal lobe during movement onset exhibited unimodal phase-lag distributions with zero mean and had highly correlated trial-by-trial values across patients, we asked whether theta oscillations in the lateral temporal lobe might reflect volume conduction from the hippocampus. Volume conduction is commonly associated with three additional characteristics: a reduction in oscillatory power with distance from the anatomical source; an increase in phase offset, relative to the anatomical source, with distance from that source; and a decrease in the magnitude of phase coupling, relative to the anatomical source, with distance from that source (36). Hence, we examined low and high theta oscillations recorded simultaneously on electrode contacts in the hippocampus and lateral temporal lobe for each of these characteristics.

First, we found no significant relationship between the anatomical distance of lateral temporal lobe electrode contacts from the hippocampus and absolute theta power; that is, theta power in the lateral temporal lobe did not decrease with distance from hippocampal contacts in either the low [$t(8) = -1.33$, $P = 0.22$] or high [$t(8) = -0.97$, $P = 0.36$] theta band, although we do note a negative trend in each case. Second, we found no consistent relationship between the anatomical distance of lateral temporal lobe electrode contacts from the hippocampus and phase offset relative to hippocampal oscillations in either the low [$t(8) = 0.82$, $P = 0.44$, $d = 0.27$] or high [$t(8) = -1.32$, $P = 0.22$, $d = 0.44$] theta band. Finally, we found that the magnitude of phase coupling with hippocampal electrode contacts did significantly decrease with anatomical distance from the hippocampus in both the low [$t(8) = -3.12$, $P < 0.05$, $d = 1.04$] and high [$t(8) = -3.85$, $P < 0.005$, $d = 1.28$] theta bands. Despite this latter result, the overall pattern of findings described here do not support the hypothesis that theta oscillations on lateral temporal lobe contacts arise as a result of volume conduction from the hippocampus. Instead, these findings are more consistent with the active entrainment of both regions by a single theta generator, although the location of that source cannot be determined from these data.

Theta Power Changes Associated with Spatial Orienting. In addition to examining changes in movement-related theta power according to the length of translational paths (Fig. 3), we also wished to ascertain whether theta power in either movement-onset or remainder-of-movement epochs was affected by the duration of the preceding stationary period, when participants may have been orienting themselves within the environment. Hence, we split the

movement-onset and remainder-of-movement epochs according to whether the duration of the immediately preceding stationary period was shorter or longer than the median duration across all trials for that patient.

For electrode contacts in the hippocampus, a repeated-measures ANOVA with levels of theta band (low versus high), movement epoch (movement onset versus remainder of movement), and duration of preceding stationary period (short versus long) revealed the expected main effect of movement epoch on theta power [$F(1,8) = 7.97$, $P < 0.05$, $\eta_p^2 = 0.50$] but no other main effects or interactions (all $P > 0.16$). Similarly, for electrode contacts in both the amygdala and lateral temporal lobe, this analysis revealed no significant main effects or interactions (all $P > 0.12$), although we do note a trend toward a main effect of movement epoch in the lateral temporal lobe [$F(1,11) = 4.24$, $P = 0.064$, $\eta_p^2 = 0.28$]. Hence, these results suggest that the duration of stationary periods immediately before movement onset, during which spatial orienting may occur, has no effect on the magnitude of theta power increases observed during either the movement-onset or remainder-of-movement epochs.

Correlations Between Theta Power and Performance. To analyze whether changes in theta power during movement onset and the remainder of movement covaried with task performance, we first split movement trials according to whether the mean Δd for the object being encoded or retrieved during that trial was above or below the median Δd across all objects during that session. For hippocampal electrode contacts, aside from the expected main effect of movement, a repeated-measures ANOVA with levels of frequency band (low versus high theta), movement epoch (movement onset versus remainder of movement), and performance (good versus bad) revealed no main effect of performance on theta power [$F(8,1) = 2.66$, $P = 0.14$, $\eta_p^2 = 0.25$] or interactions (all $P > 0.55$). Similarly, for lateral temporal lobe electrode contacts, this analysis revealed no main effect of performance on theta power [$F(11,1) = 0.64$, $P = 0.44$, $\eta_p^2 = 0.06$] or interactions (all $P > 0.31$). Second, we split movement trials during the retrieval period according to whether performance on that trial was above or below the median trial by the trial Δd for that session, but a repeated-measures ANOVA again revealed no effect of performance on theta power in the hippocampus [$F(8,1) = 0.24$, $P = 0.64$, $\eta_p^2 = 0.03$] and no interactions (all $P > 0.51$). Similarly, for lateral temporal lobe electrode contacts, this analysis revealed no effect of performance on theta power [$F(11,1) = 1.99$, $P = 0.19$, $\eta_p^2 = 0.15$] and no interactions (all $P > 0.08$). These findings suggest that movement-related theta power increases are not predictive of spatial memory performance in this task.

Theta Power Changes Associated with Button Pressing. There is a possibility that the analyses of movement-related changes in oscillatory power presented in the main text were confounded by button pressing, as patients must hold a button to move across the virtual environment but not to remain stationary (*SI Materials and Methods*). To address this issue, we analyzed EEG data from response periods during retrieval trials in the spatial memory task when a button was pressed to indicate remembered object locations. Importantly, these response periods most often occurred during stationary periods, allowing us to disambiguate the oscillatory correlates of button pressing and translational movement. Hence, we analyzed mean z-scored power in the low and high theta band during a −0.5:0.5-s window around each response button press, excluding any trials in which participants were moving during that 1-s period (in addition to any trials containing IIS or other artifacts).

For electrode contacts in the hippocampus (mean ± SD = 23.7 ± 10.7 trials per patient), mean z-scored power during response periods was not different from zero in either the low [$t(8) = 1.31$, $P = 0.23$, $d = 0.44$] or high [$t(8) = -0.62$, $P = 0.55$, $d = 0.21$] theta band (Fig. S4 *A* and *B*). Similarly, for electrode contacts in the amygdala (21.8 ± 11.0 trials per patient) and lateral temporal lobe (27.1 ± 11.0 trials per patient) (Fig. S4*C*), we identified no significant changes in low or high theta power during response periods (all $P > 0.54$) (Fig. S4*D*). Hence, we conclude that the changes in movement-related theta power shown in Fig. 2 cannot be attributed to button pressing.

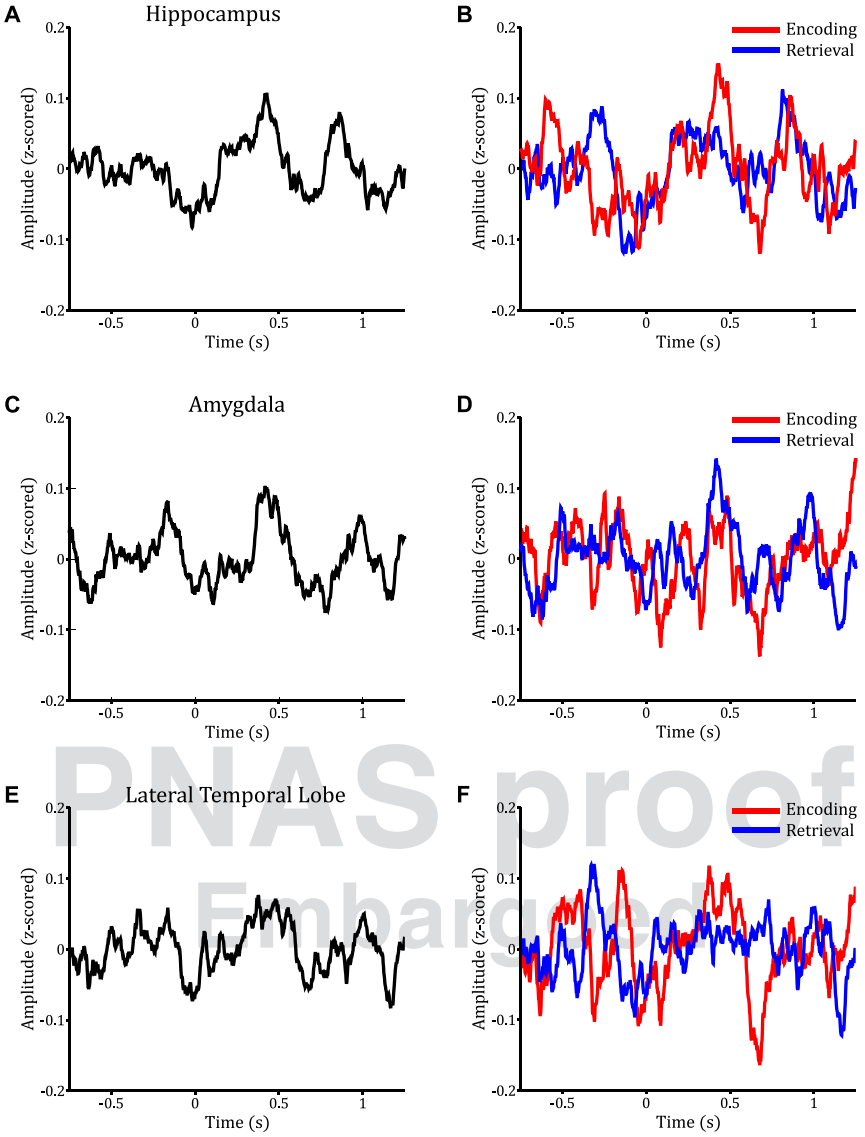

Fig. S1. ERPs at virtual movement onset averaged across all movement-onset trials (*Left*) and separated by encoding and retrieval phases (*Right*) in the hippocampus (*A* and *B*); amygdala (*C* and *D*), and lateral temporal lobe (*E* and *F*).

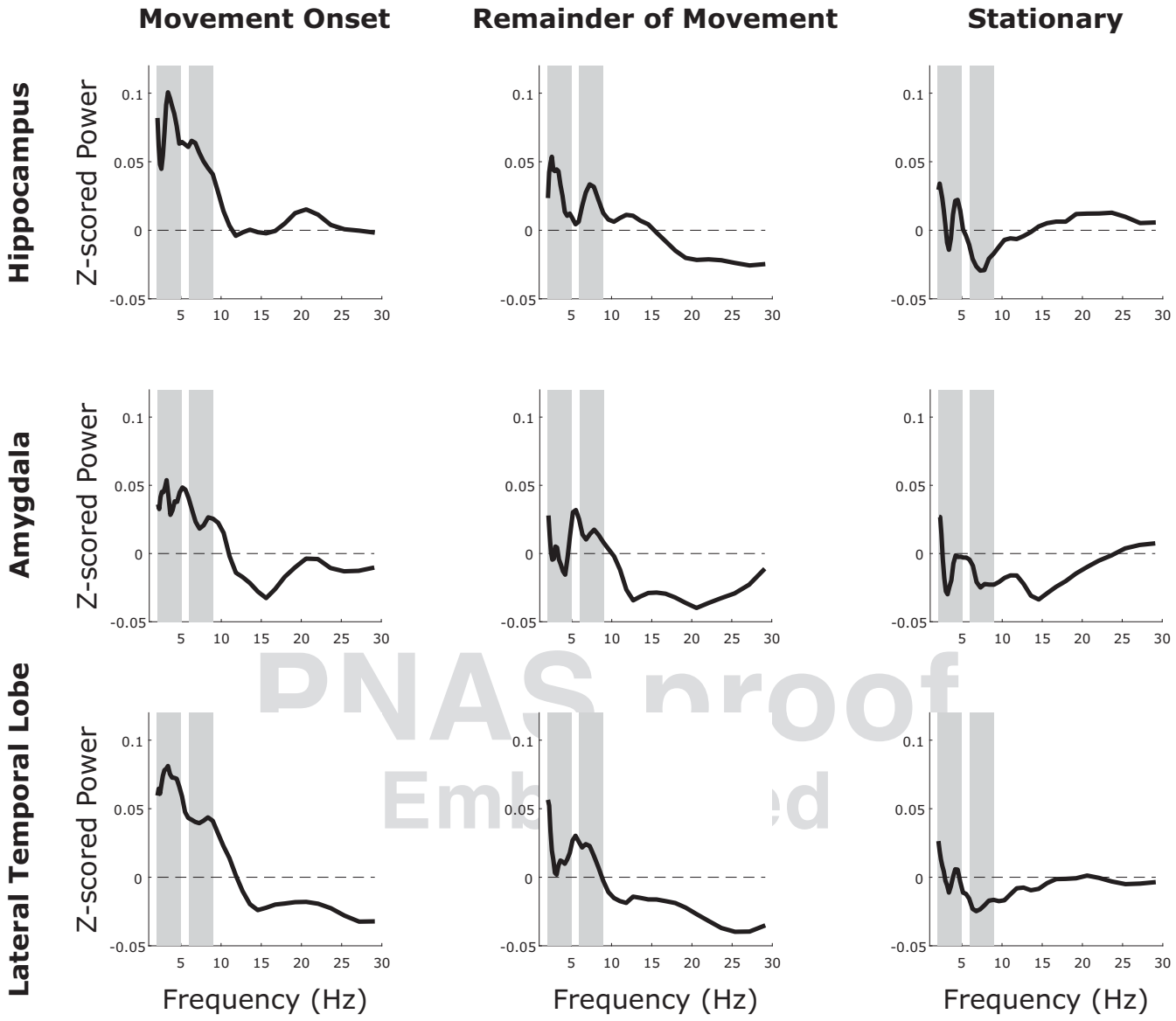

Fig. S2. Individual power spectra for electrode contacts in each cortical region and each movement condition, with low (2–5 Hz) and high (6–9 Hz) theta bands highlighted with light gray bars. Peaks in both the low and high theta bands are generally visible across movement-onset conditions, while peaks in the low theta band are visible only during stationary periods. In addition, low-frequency (<10 Hz) power is generally greater during movement onset than during either remainder-of-movement or stationary periods.

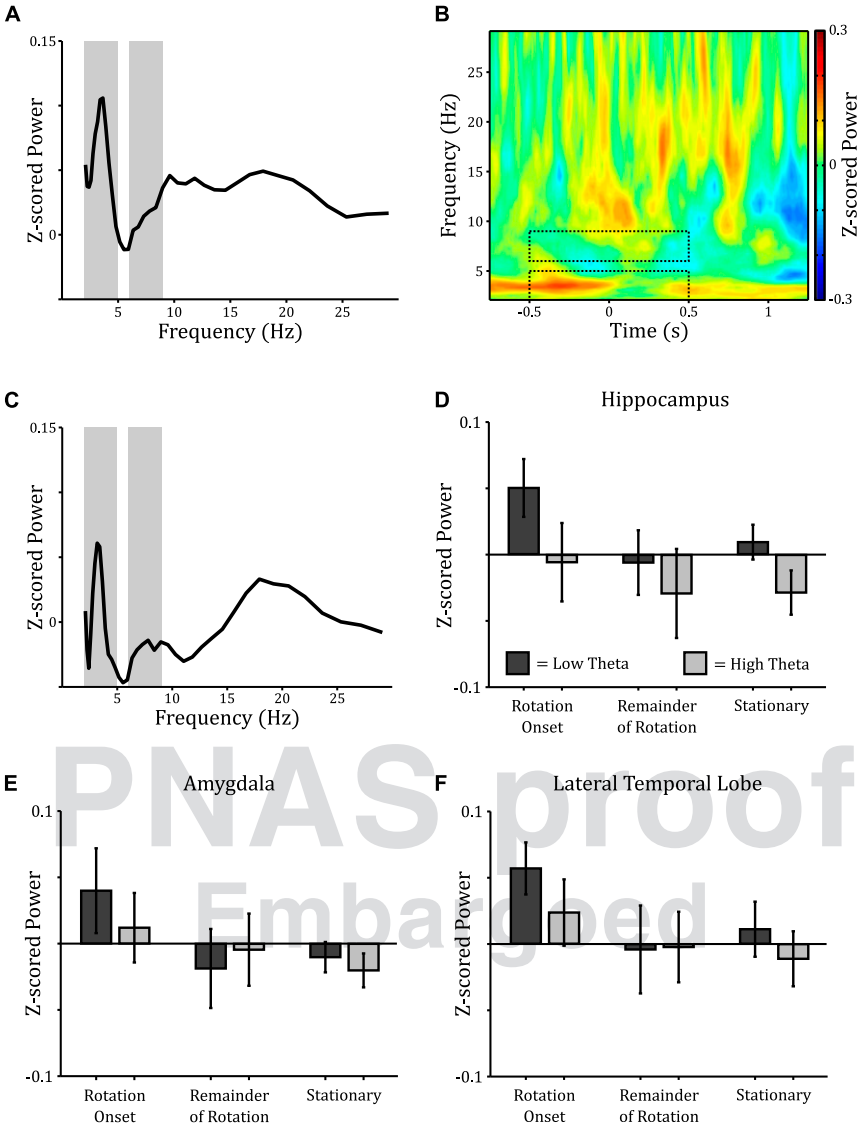

Fig. S3. Theta power changes during rotational movement across the temporal lobe. (*A*) Average power spectrum for rotation-onset epochs (mean ± SD = 53.3 ± 38.3 trials per patient), baseline corrected by the mean power at each frequency during stationary periods (89.5 ± 76.2 trials per patient lasting 2.33 ± 0.51 s), for electrode contacts in the hippocampus. Low (2–5 Hz) and high (6–9 Hz) theta bands are marked in gray. (*B*) Spectrogram of power around rotation onset, baseline corrected by mean power at each frequency during stationary periods, for electrode contacts in the hippocampus. Black dashed regions indicate the low and high theta bands for the 1-s period around rotation onset. (*C*) Average power spectrum for remainder-of-rotation epochs (36.6 ± 26.1 trials per patient lasting 2.0 ± 0.16 s), baseline corrected by the mean power at each frequency during stationary periods, for electrode contacts in the hippocampus. Peaks in the low and high theta bands (marked in gray) are visible but are less pronounced than during movement onset. (*D*–*F*) Mean z-scored power in the low (2–5 Hz) and high (6–9 Hz) theta bands during rotation-onset, remainder-of-rotation, and stationary epochs in the hippocampus (*D*), amygdala (61.3 ± 29.0 rotation-onset trials, 39.0 ± 19.5 remainder-of-rotation trials lasting 2.2 ± 0.3 s, and 97.8 ± 60.3 stationary trials lasting 2.55 ± 0.55 s per patient) (*E*), and lateral temporal lobe (62.6 ± 33.2 rotation-onset trials, 40.9 ± 22.0 remainder-of-rotation trials lasting 2.18 ± 0.25 s, and 102.0 ± 66.2 stationary trials lasting 2.46 ± 0.52 s per patient) (*F*). There are no significant changes in either low or high theta power across any of these epochs in any cortical region (all $P > 0.08$).

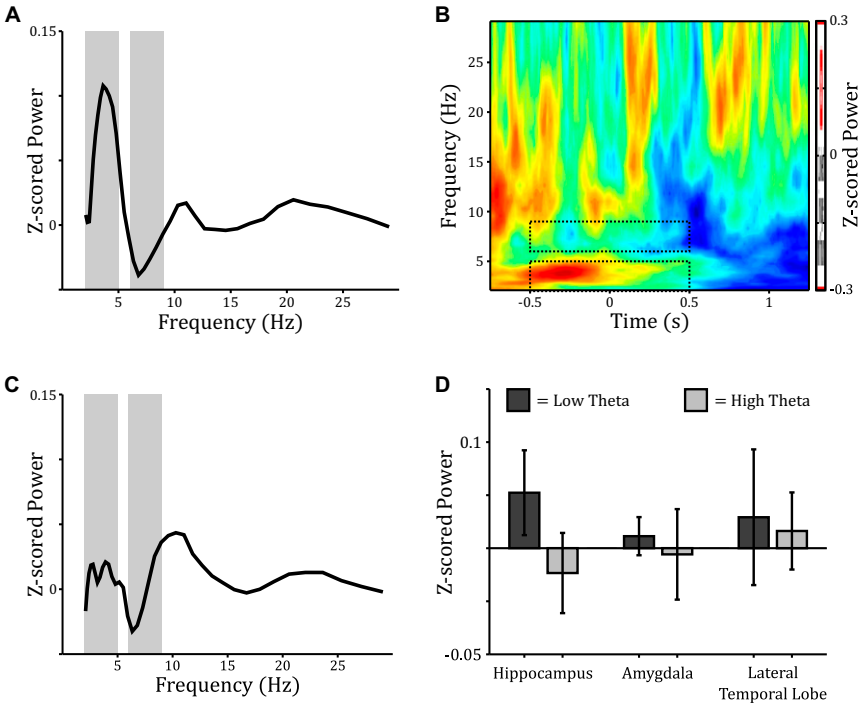

Fig. S4. Theta power changes during button pressing. (*A*) Spectrum of mean z-scored power versus frequency on hippocampal electrodes during 1-s response periods, which correspond to button pressing in the absence of translational movement. Low (2–5 Hz) and high (6–9 Hz) theta bands are marked in gray. (*B*) Spectrogram of z-scored power on hippocampal electrodes around button pressing in the absence of translational movement. Black dashed regions indicate the low and high theta bands for the 1-s response period. (*C*) Spectrum of mean z-scored power versus frequency on lateral temporal lobe electrodes during 1-s response periods, which correspond to button pressing in the absence of translational movement. Low (2–5 Hz) and high (6–9 Hz) theta bands are marked in gray. (*D*) Comparison of mean z-scored power in the low (dark gray) and high (light gray) theta bands on electrode contacts in the hippocampus, amygdala, and lateral temporal lobe during a 1-s period around button pressing. There are no significant changes in either high or low theta power in any region.

Table S1. General details of the patient population

Patient ID	Age, y	Handed	Gender	Implanted hemisphere	Sessions completed	Hippocampal contacts	Amygdalar contacts	Lateral temporal lobe contacts
1	21	R	F	R	2	4	0	6
2	28	R	M	L	1	0	2	2
3	44	R	F	R	2	5	2	8
4	41	L	M	R	1	5	2	9
5	26	R	M	R	2	5	3	8
6	21	R	M	L	2	2	3	5
7	22	R	M	L	2	0	3	8
8	37	R	F	R	2	4	3	10
9	30	R	F	Bilateral	2	8	4	12
10	20	L	F	R	2	5	3	9
11	28	R	M	R	1	5	2	8
12	29	R	M	L	2	0	3	0
13	23	R	F	R	1	0	2	2

Table S2. Clinical details of the patient population

Patient ID	Age at first seizure	Language dominance	Seizure onset zone	Surgical outcome	Hippocampal damage?	Additional notes
1	14 y	L	Right MTL	Right MTL resection	Right hippocampal sclerosis, severe neuronal loss in CA1	Right parietal gyral calcification
2	22 y	L	Left mesial orbito-frontal	No surgery	None	
3	23 y	L	Right MTL	Right MTL resection	End folium sclerosis of the right hippocampus	
4	25 y	L	Right MTL	Right MTL resection	Right hippocampal sclerosis, severe neuronal loss in CA1	Periventricular heterotopia
5	13 y	B	Right neocortical TL	Right neocortical TL resection	None	
6	12 mo	B	Left occipito-parietal	Left occipito-parietal resection	None	Focal cortical dysplasia IIA
7	11 y	L	Left occipito-parietal	Left occipito-parietal resection	None	Focal cortical dysplasia IIID
8	21 y	L	Right temporal-occipital	DNT removal from right temporal-occipital cortex	None	
9	23 y	L	Bilateral MTL	No surgery	None	Small left occipito-temporal sulcus lesion
10	6 y	L	Right TPJ and MTL	Right MTL resection	None	
11	8 y	L	Right neocortical TL	No surgery	None	Right temporal/parietal cortical dysplasia, polymicrogyria
12	15 y	L	Left insula	No surgery	None	
13	3 y	L	Left frontal lobe	No surgery	None	

DNT, dysembryoplastic neuroepithelial tumor; MTL, medial temporal lobe; TL, temporal lobe; TPJ, temporoparietal junction.

Table S3. Number of trials in each task epoch for patients with depth electrodes in the hippocampus

Patient ID	Encoding movement-onset trials	Retrieval of movement-onset trials	Encoding remainder-of-movement trials	Mean length, s	Retrieval of remainder-of-movement trials	Mean length, s	Encoding stationary trials	Mean length, s	Retrieval of stationary trials	Mean length, s
1	10.0	7.8	7.0	3.0	6.8	1.8	5.8	1.4	26.3	1.9
3	40.2	70.4	31.2	1.9	52.6	2.1	28.6	1.6	89.8	1.9
4	9.2	27.2	2.8	1.4	13.8	1.9	23.6	2.5	59.2	2.9
5	18.6	9.4	13.6	2.0	6.4	2.0	17.0	2.5	6.4	1.5
6	57.0	140.0	39.0	1.8	102.5	2.0	46.5	1.8	174.0	2.4
8	36.8	90.0	22.8	1.8	44.5	1.9	55.5	3.0	144.3	3.4
9	7.5	17.6	7.4	1.8	12.0	2.3	8.5	2.1	11.8	2.0
10	18.8	41.6	7.4	1.3	28.0	1.6	16.2	2.0	63.6	1.9
11	7.4	15.6	5.8	1.5	8.8	1.3	9.0	1.9	19.4	3.2
Mean	22.8	46.6	15.2	1.8	30.6	1.9	23.4	2.1	66.1	2.3
Maximum	57	140	39	3	102.5	2.3	55.5	3	174	3.4
Minimum	7.4	7.8	2.8	1.3	6.4	1.3	5.8	1.4	6.4	1.5

Table S4. Number of trials in each task epoch for patients with depth electrodes in the amygdala

Patient ID	Encoding movement-onset trials	Retrieval of movement-onset trials	Encoding remainder-of-movement trials	Mean length, s	Retrieval of remainder-of-movement trials	Mean length, s	Encoding stationary trials	Mean length, s	Retrieval of stationary trials	Mean length, s
2	13.0	33.5	11.5	1.8	17.0	1.5	13.5	2.6	55.5	2.3
3	40.0	71.5	29.5	1.9	53.5	2.1	29.0	1.6	91.0	1.9
4	13.0	35.0	5.0	1.4	19.0	2.0	43.0	2.5	90.0	3.1
5	19.5	10.0	14.5	2.0	7.0	2.0	17.0	2.5	8.0	1.8
6	52.3	119.0	38.3	1.7	81.3	2.0	42.3	1.9	134.7	2.3
7	27.3	27.3	26.0	2.0	14.3	2.5	26.0	3.8	65.3	2.6
8	43.3	95.3	27.3	1.8	45.3	1.9	64.7	2.9	159.7	3.4
9	7.3	17.5	7.3	1.7	12.3	2.3	8.8	2.1	11.8	2.1
10	19.0	51.0	8.7	1.4	33.3	1.6	16.7	1.8	64.0	2.0
11	10.5	22.0	8.0	1.7	14.5	1.3	11.5	1.8	31.5	3.8
12	21.0	41.0	20.0	2.1	31.0	2.0	25.3	2.1	85.0	3.5
13	22.0	42.0	16.0	1.9	36.0	1.6	17.0	1.5	62.0	2.4
Mean	24.0	47.1	17.7	1.8	30.4	1.9	26.2	2.3	71.5	2.6
Maximum	52.3	119	38.3	2.1	81.3	2.5	64.7	3.8	159.7	3.8
Minimum	7.3	10	5	1.4	7	1.3	8.8	1.5	8	1.8

Table S5. Number of trials in each task epoch for patients with depth electrodes in the lateral temporal lobe

Patient ID	Encoding movement-onset trials	Retrieval of movement-onset trials	Encoding remainder-of-movement trials	Mean length, s	Retrieval of remainder-of-movement trials	Mean length, s	Encoding stationary trials	Mean length, s	Retrieval of stationary trials	Mean length, s
1	20.0	20.0	19.5	2.6	21.2	1.9	7.7	1.4	62.5	2.0
2	13.0	33.0	11.0	1.8	17.0	1.5	14.0	2.6	56.5	2.4
3	42.1	72.8	33.0	2.0	55.8	2.1	29.0	1.6	95.6	2.0
4	12.2	34.1	4.4	1.3	18.7	2.0	42.0	2.5	89.1	3.1
5	18.6	10.0	15.3	2.2	6.4	2.0	17.4	2.4	6.6	1.5
6	58.0	135.4	38.2	1.7	93.6	1.9	50.8	1.9	165.8	2.4
7	33.8	36.6	29.8	1.9	24.0	2.4	38.4	5.1	82.9	2.5
8	42.5	94.5	25.6	1.9	47.2	1.8	60.0	2.9	158.2	3.4
9	7.9	18.9	7.9	1.9	12.9	2.2	8.8	2.1	12.6	2.0
10	26.2	55.0	11.9	1.5	34.3	1.7	20.9	2.1	91.8	2.1
11	9.0	19.6	6.0	1.5	13.3	1.3	10.3	1.9	23.8	3.4
13	22.0	42.0	16.0	1.9	37.0	1.6	17.0	1.5	62.5	2.4
Mean	25.4	47.7	18.2	1.9	31.8	1.9	26.4	2.3	75.7	2.4
Maximum	58	135.4	38.2	2.6	93.6	2.4	60	5.1	165.8	3.4
Minimum	7.9	10	4.4	1.3	6.4	1.3	7.7	1.4	6.6	1.5